



Single Event Resolution of Plant Plasma Membrane Protein Endocytosis by TIRF Microscopy

Alexander Johnson and Grégory Vert*

Institute for Integrative Biology of the Cell (I2BC), CNRS/CEA/Univ. Paris-Sud, Université Paris-Saclay, Gif-sur-Yvette, France

Endocytosis is a key process in the internalization of extracellular materials and plasma membrane proteins, such as receptors and transporters, thereby controlling many aspects of cell signaling and cellular homeostasis. Endocytosis in plants has an essential role not only for basic cellular functions but also for growth and development, nutrient delivery, toxin avoidance, and pathogen defense. The precise mechanisms of endocytosis in plants remain quite elusive. The lack of direct visualization and examination of single events of endocytosis has greatly hampered our ability to precisely monitor the cell surface lifetime and the recruitment profile of proteins driving endocytosis or endocytosed cargos in plants. Here, we discuss the necessity to systematically implement total internal reflection fluorescence microscopy (TIRF) in the Plant Cell Biology community and present reliable protocols for high spatial and temporal imaging of endocytosis in plants using clathrin-mediated endocytosis as a test case, since it represents the major route for internalization of cell-surface proteins in plants. We developed a robust method to directly visualize cell surface proteins using TIRF microscopy combined to a high throughput, automated and unbiased analysis pipeline to determine the temporal recruitment profile of proteins to single sites of endocytosis, using the departure of clathrin as a physiological reference for scission. Using this ‘departure assay’, we assessed the recruitment of two different AP-2 subunits, alpha and mu, to the sites of endocytosis and found that AP2A1 was recruited in concert with clathrin, while AP2M was not. This validated approach therefore offers a powerful solution to better characterize the plant endocytic machinery and the dynamics of one’s favorite cargo protein.

OPEN ACCESS

Edited by:

Jiri Friml,
Institute of Science and Technology,
Austria

Reviewed by:

Sen Subramanian,
South Dakota State University, USA
Yuhui Chen,
Samuel Roberts Noble Foundation,
USA

*Correspondence:

Grégory Vert
gregory.vert@i2bc.paris-saclay.fr

Specialty section:

This article was submitted to
Technical Advances in Plant Science,
a section of the journal
Frontiers in Plant Science

Received: 16 November 2016

Accepted: 04 April 2017

Published: 24 April 2017

Citation:

Johnson A and Vert G (2017) Single
Event Resolution of Plant Plasma
Membrane Protein Endocytosis by
TIRF Microscopy.
Front. Plant Sci. 8:612.
doi: 10.3389/fpls.2017.00612

Keywords: imaging techniques, endocytosis, TIRF microscopy, Arabidopsis, plants, trafficking

INTRODUCTION

Endocytosis is the process of transporting cell surface or extracellular materials, including proteins, lipids and nutrients, into the cell *via* invaginations of small vesicles that pinch off from the plasma membrane. While there are many different forms of endocytosis, the most characterized is clathrin-mediated endocytosis (CME). It is defined by a coat of clathrin which forms around the invaginating vesicle. At least 60 key endocytosis accessory proteins (EAPs) are conserved between mammalian and yeast CME (Merrifield and Kaksonen, 2014). Some of these key EAPs also have homologs in plants, suggesting that plant CME might use the same mechanisms as these other systems (Baisa et al., 2013).

CME is best understood in mammalian and yeast systems (McMahon and Boucrot, 2011; Lu et al., 2016) where over 60 conserved key EAPs have been characterized and for which details of the physiological role and precise temporal dynamics are defined (McMahon and Boucrot, 2011; Merrifield and Kaksonen, 2014; Lu et al., 2016). These findings have shown that CME can be broken down into five distinct steps; nucleation, cargo selection, coat assembly, scission, and uncoating. Each stage requires a different subset of EAPs to facilitate the overall propagation of creating a vesicle from the plasma membrane.

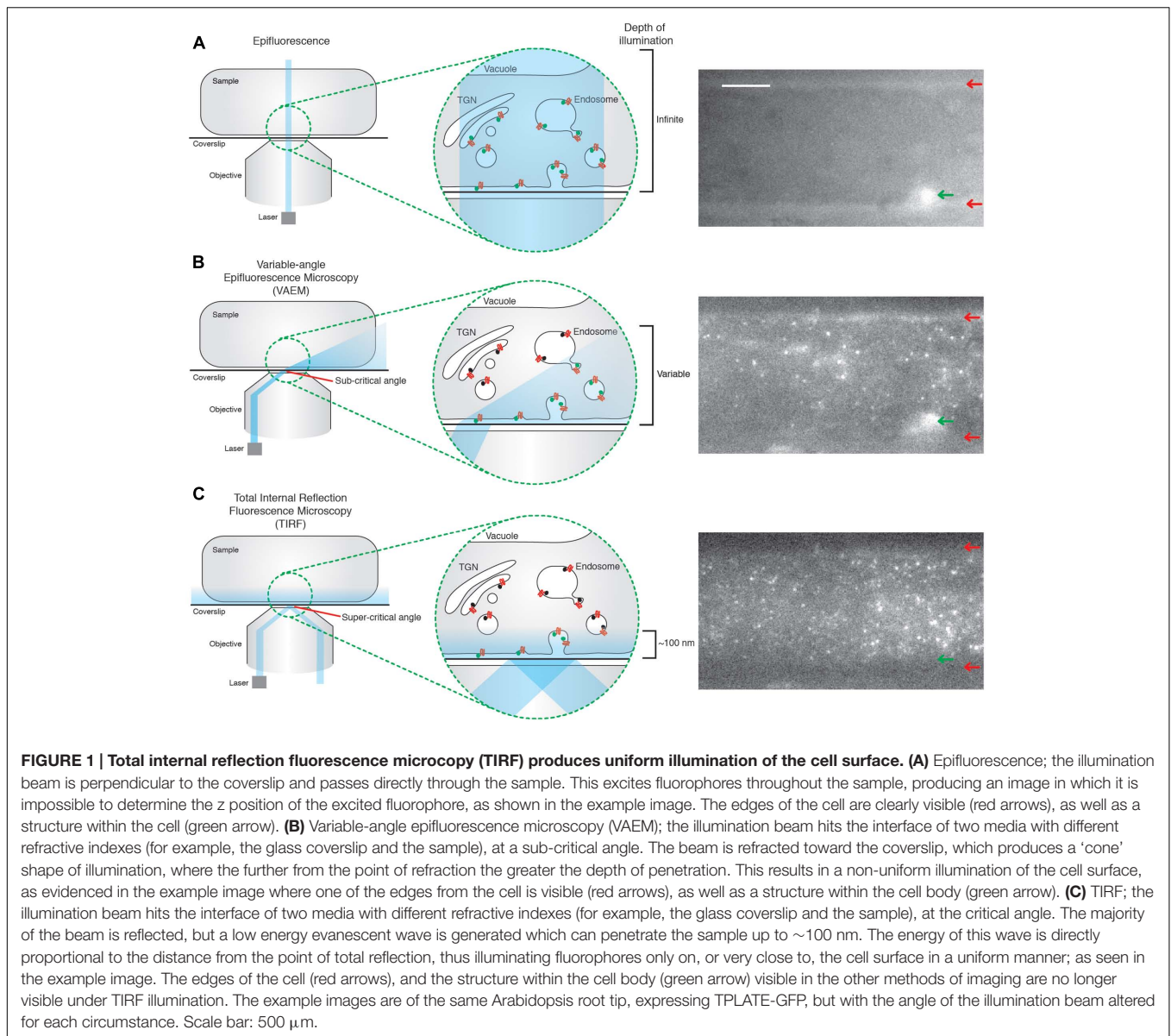
In the past few years, a number of plant plasma membrane proteins have been shown to utilize the CME pathway. These include the some of the PIN auxin efflux carrier and the PIP2 aquaporin (Dhonukshe et al., 2007), subunits of the cellulose synthase (Bashline et al., 2013), the IRT1 root iron transporter (Barberon et al., 2014), and the plant steroid hormone receptor BRI1 (Di Rubbo et al., 2013; Martins et al., 2015), among others. In contrast to mammalian and yeast systems, little is known about CME in plants and at present, there are only a handful of reports which really begin to address the precise molecular mechanisms of plant CME. Identification of plant EAP homologs of mammalian or yeast EAPs (Chen et al., 2011; Baisa et al., 2013) has led to genetic manipulations of CME to demonstrate that some of the EAP homologs are indeed key proteins for plant CME. For example, use of clathrin heavy chain mutants interfered with the recycling and polarization of PIN proteins, thus demonstrating that CME is indeed important in cell surface processes (Kitakura et al., 2011). All the canonical Adaptor Protein 2 (AP-2) subunits are also conserved in plants (Happel et al., 2004; Chen et al., 2011; Yamaoka et al., 2013), and also appear to be important for the internalization of some cell surface reporters and normal plant development (Bashline et al., 2013; Di Rubbo et al., 2013; Fan et al., 2013; Kim et al., 2013). However, there are some key proteins which appear to have not been conserved between plants and other model systems (Gadeyne et al., 2014; Zhang et al., 2015), suggesting that CME in plants is partly reliant upon unique plant EAPs, and therefore potentially utilizes different mechanisms of CME.

One of the main reasons mammalian and yeast systems enjoy such detailed physiological characterization of CME compared to plants is the use of specific technologies which allow direct examination of single events of CME *in vivo*. Much of the current characterization of plant CME has relied heavily upon indirect, and often static, biochemical and pharmacological approaches using confocal microscopy that fail to capture the often subtle roles of EAPs at CME sites with any temporal resolution (Aguet et al., 2013). Single event resolution is, however, critical for defining precise physiological roles for the EAPs, as it directly tracks and allows quantification of the dynamics of EAPs at the site of their physiological action. One of the key technologies facilitating single event imaging of CME is total internal reflection fluorescent microscopy (TIRF). This method of imaging makes use of a low energy evanescent wave which is generated when the illumination laser undergoes total reflection at the interface of two different media of different reflective indexes; for example, between a coverslip and imaging

medium (Axelrod, 2001). The energy of the evanescent wave is directly proportional to the distance away from the point of reflection, typically penetrating samples up to 100 nm. TIRF therefore only excites fluorophores on, or very close to the cell surface (Axelrod, 2001). This property makes of TIRF a great method to image cell surface processes such as CME. This is in contrast to traditional epifluorescence approaches, where the illumination source passes directly through the whole sample, thereby stimulating fluorophores present on structures deeper within the cell and making it impossible to determine if the fluorescent signal originates from the cell surface (**Figure 1A**). To overcome the drawbacks of epifluorescence, spinning disk confocal microscopy has often been used in the plant field to look at cell surface processes. Use of the pinholes allows one to select the cell surface plane and facilitates rapid acquisition. However, due to the nature of the pinholes, a lot of photons are discarded and the z-resolution is still limited to ~500 nm. This makes spinning disk microscopy unsuitable for tracking weak signals and focusing with great precision on cell surface EAPs aggregating at sites of CME (Mettlen and Danuser, 2014).

Another approach to image the plant cell surface is the variable angle evanescent microscopy (VAEM), also called 'pseudo-TIRF'. VAEM relies on refraction, rather than reflection as in TIRF, of the illumination laser at the interface of two different media of different reflective indexes (Konopka et al., 2008). The illumination wave is refracted to almost parallel angles to the coverslip, thus exciting fluorophores near the coverslip. However, the depth of penetration of the refracted wave is not uniform across the sample (**Figure 1B**). The further away from the point of reflection, the broader the illumination beam is, thus allowing deeper stimulation of fluorophores within the cell (Wan et al., 2011). This non-uniform illumination allows one to distinguish between TIRF and VAEM while imaging (**Figures 1B,C**). TIRF is therefore more sensitive, produces evenly illuminated images with a higher signal to noise ratio allowing the tracking of weaker signals, and is more accurate to quantify cell surface lifetime due to uniform z-resolution. As such, TIRF is now seen as the standard method for CME investigation in both mammalian and yeast systems, despite yeast having a cell wall (Rappoport, 2008; Loerke et al., 2009). Encouragingly, a handful of studies showed that TIRF is now possible in plants (Vizcay-Barrena et al., 2011; Wan et al., 2011).

Along with specific cell surface imaging techniques, automated image analysis algorithms have been developed, which allowed high throughput, unbiased and rapid analysis of CME TIRF images (Jaqaman et al., 2008; Aguet et al., 2013; Langhans and Meckel, 2014). Thousands of fluorescent signals can be automatically detected, tracked and quantified from a time-lapse movie of the cell surface in under an hour. This has allowed the analysis of huge datasets and thus accurately depicted CME with a high power of statistical significance (Loerke et al., 2009). Although a few recent studies in plants have used such algorithms (Wang et al., 2015), the vast majority rely on manual analysis methods using ImageJ (Konopka et al., 2008; Bashline et al., 2013; Martins et al., 2015). This mostly involves making kymographs of a time-lapse TIRF or VAEM



movie and manually measuring each line of fluorescence in ImageJ. This is a very time-consuming endeavor, and can take months to produce small datasets. Furthermore, this technique is not as sensitive at detecting particles as a computer algorithm, and is open to selection bias toward the brighter or persisting signals. Manual tracking is also unsuitable for proteins which are dense on the cell surface, as there is too much noise to accurately measure single traces of proteins.

Taking together that TIRF is indeed possible in plants and that plant images are suitable for automated particle detection programs, we developed a reliable method for directly studying single events of CME in plants with high temporal and spatial resolution. We established a protocol for allowing TIRF imaging to be performed on the Arabidopsis root tip and successfully applied single endocytic event detection

and tracking scripts to the images to allow rapid, high throughput and unbiased calculation of the cell lifetime of key EAPs. Finally, we detailed the development of a dual channel physiological departure assay, which allows the fine characterization of EAPs at single sites of CME. Altogether, this provides the plant endocytosis community with powerful imaging pipelines to greatly increase our understanding of plant CME, thus bridging the gap in knowledge between other model systems.

MATERIALS AND METHODS

Plant Material

Plants expressing AP2A1-GFP (35S::AP2A1-GFP) were gifted from Dr. Russinova (VIB, Belgium). CLC-tagRFP

(pRPS5A::CLC2-tagRFP) and TPLATE-GFP (pLat52::TPLATE-GFP) were gifted from Dr. Van Damme (VIB, Belgium). AP2M-YFP (pAP2M::AP2M-YFP) was gifted by Dr. Gu (Pennsylvania State University, USA). CLC-GFP (pCLC::CLC2-GFP) was provided by Dr. Lin (Chinese Academy of Sciences, Beijing, China). DRP1c-GFP (pDRP1c::DRP1c-GFP) was gifted by Dr. Bednareck (University of Wisconsin, USA).

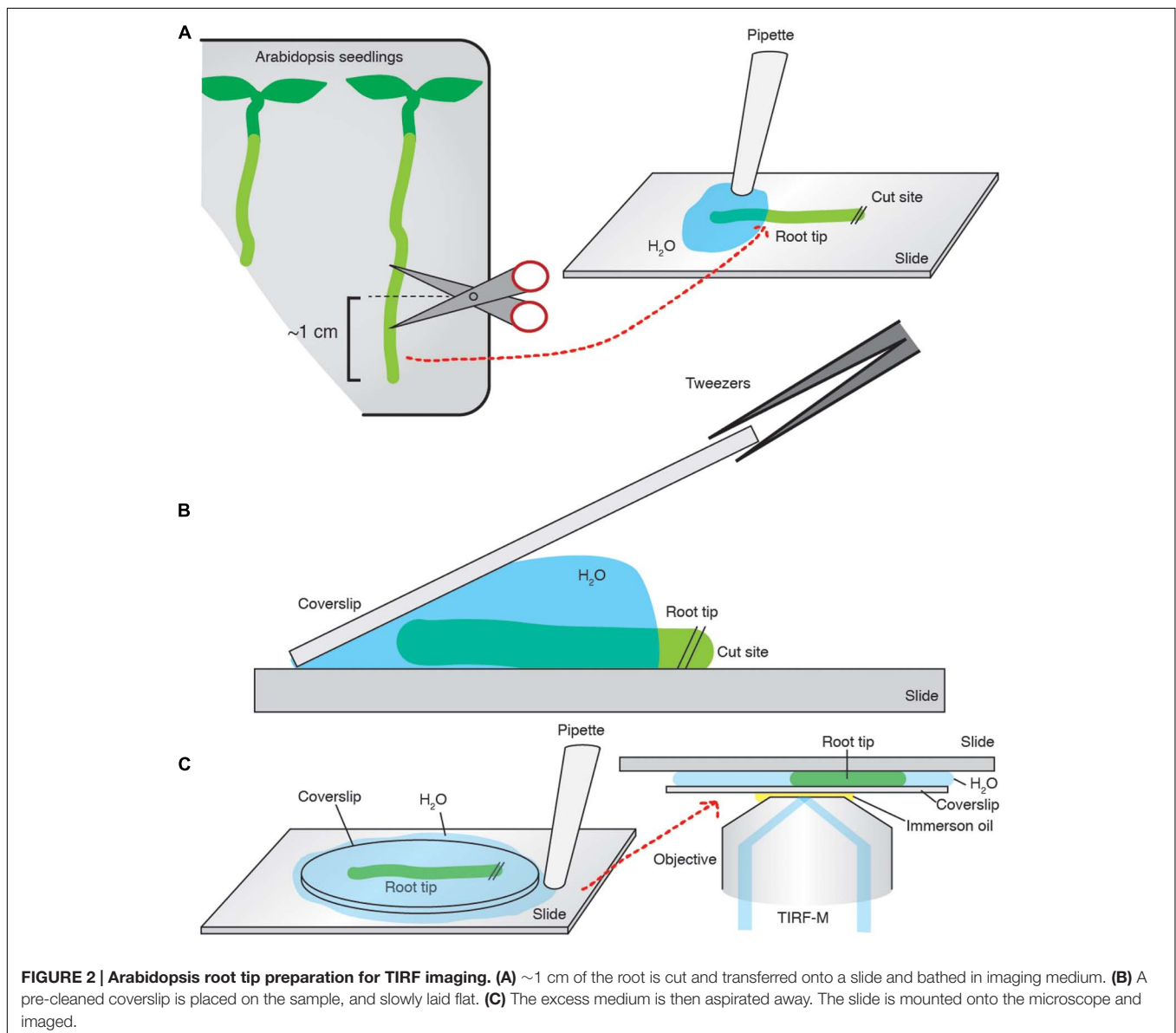
For dual color analysis, plants expressing the EAPs fused to GFP were crossed with the pollen from CLC-tagRFP plants, and the F1 progenies were used.

Growth Conditions

Plants were plated on half-strength Linsmaier and Skoog medium ($1/2$ LS) and incubated in the dark at 4°C for 2–4 days. Plates were transferred to a heated light chamber (21°C with cycles of 16 h light/8 h dark) and incubated for 10 days prior to imaging.

TIRF Imaging and Analysis

Total internal reflection fluorescent microscopy samples were prepared in the following manner. Coverslips (Borosilicate glass, thickness 1, from VWR) were cleaned with a 0.01% (w/v) Decon 90, 100 mM NaOH solution and then sequentially washed with ddH₂O, 100% ethanol and then acetone. The root of interest was cut to ~ 1 cm above the root tip, and transferred to a microscope slide where it was bathed in an excess of imaging medium before a pre-cleaned coverslip was placed on top of the sample. The excess medium was then aspirated to create a compression of the coverslip onto the sample, ensuring that the epidermal cells were in direct contact with the coverslip and that the root was immobilized without damage. The slide was subsequently mounted onto a Nikon Eclipse Ti microscope equipped with a Nikon APO TIRF 100/1.49 oil immersion objective (Figure 2). The excitation wavelengths used were

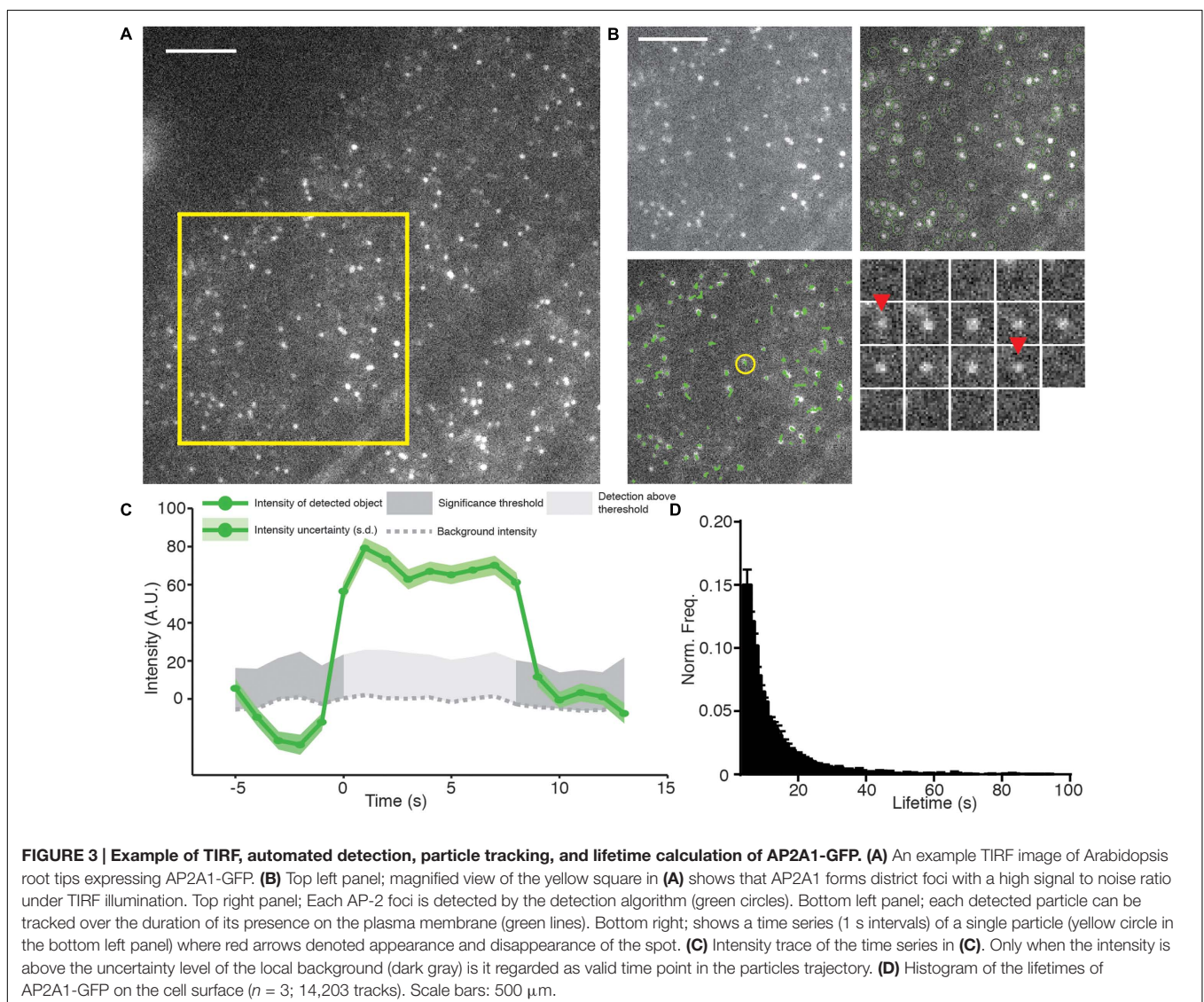


491 nm and, or, 561 nm for GFP and tagRFP, respectively, provided by a 100-mW diode laser Toptica AOTF. An emission filter Chroma ET 405/491/561/642 was used in conjunction with a Coolsnap HQ2 camera (photometrics).

For single channel analyses, images were acquired at 1 s intervals, for a duration of 5 min. The time-lapse movies were subjected to only the particle detection and tracking algorithms from the *cmeAnalysis* package (Aguet et al., 2013) using Matlab 2013b (Mathworks). Using customized homemade Matlab scripts (available upon request), the complete raw trajectories were screened so that only tracks which had both a duration greater than 5 s and that lasted less than the total length of the movie, and tracks which were not present in the first of last five frames of the movie were included in the cell surface lifetime calculation. The data from multiple experiments were combined to produce cell surface lifetime values.

Dual channel time-lapse movies were acquired sequentially at 500 ms intervals, at an interval of 1 s per channel, for a duration of

5 min. Each channel was subjected only to the particle detection and tracking stages of the *cmeAnalysis* package in Matlab 2013b (Mathworks), as described above. Custom homemade Matlab scripts (available upon request) were used to examine if the raw *cmeAnalysis* trajectories of each channel overlapped. If a 1 frame overlap was found, the different channel trajectories were paired. Paired trajectories were subjected to the departure analysis if the appearance and disappearance of the secondary channel trajectory of each channel were within 5 s of the reference channel trajectory's appearance and disappearance (Aguet et al., 2013). The mean lifetime value of these paired trajectories was calculated, and paired trajectories where the reference trajectory lifetime equaled this value (± 1 s) were combined and aligned to the moment of the disappearance of the reference channel, thus creating a departure trace. The mean departure traces from multiple experiments were combined, normalized and plotted to produce a robust recruitment profile of the EAP of interest to the moment of the departure of the reference signal.



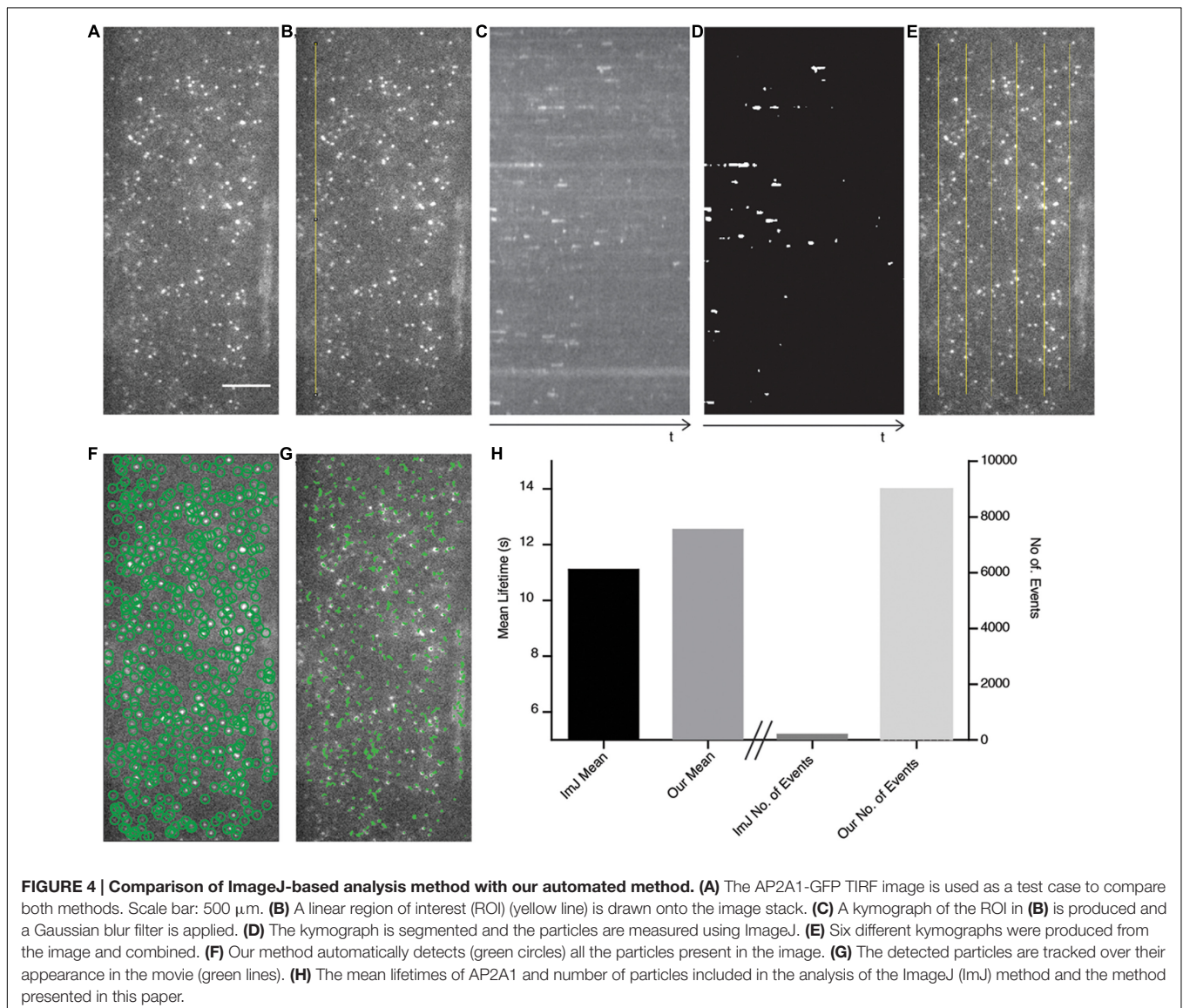
RESULTS AND DISCUSSION

Establishing TIRF, Automated Particle Detection, and Tracking Analysis in Arabidopsis Roots

The use of TIRF in plants is relatively new and there have been only a few reports precisely detailing how it is achieved. We therefore set out to establish and share a reliable and reproducible method for TIRF imaging and analyzing TIRF data in the Arabidopsis root. As the evanescent wave only penetrates depths up to 100 nm (Axelrod, 2001), a major requirements of TIRF is mounting the sample so it is in direct contact with the coverslip. We developed a simple method for successfully mounting Arabidopsis roots onto cover slips, which ensures contact of the epidermal cells with the coverslip and immobilization without damaging the sample (Figure 2).

While imaging an intact system provides analysis of CME in its physiological context, it also presents difficulty in selecting the same cell type and developmental stage. To overcome this, we use the lateral root cap as a reference point. The first suitable epidermal cells generating TIRF images, usually located 5–13 cells up from the end of the lateral root cap, were selected for analyses.

Plants expressing a GFP labeled alpha subunit of the canonical CME AP-2 adaptor protein (AP2A1-GFP) were subjected to TIRF using these methods (Figure 3A). AP2A1-GFP forms discrete foci on the cell surface, as expected, and these spots have a high signal to noise ratio. Importantly, the image has a uniform intensity across the whole sample, indicating that TIRF illumination was used. Once a suitable cell is selected, a time-lapse movie is acquired with a time interval between frames of 1 s for a duration of 5 min. The movie is then subjected to automated particle detection and tracking. To do this, we used only the



detection and tracking parts of the *cmeAnalysis* package (Aguet et al., 2013). The *cmeAnalysis* package was selected for use as it outperforms other detection and tracking programs available, like *uTrack* and *Imaris* (Mettlen and Danuser, 2014). It uses a model fitting mode of detection, which allows the use of statistical test to determine if an object fits the expected point spread function of the specific fluorophore used, and if the fluorescent intensity is statistically significant compared to the local background (Aguet et al., 2013). *cmeAnalysis* detected AP2A1-GFP spots with a very high degree of accuracy (Figure 3B).

The *cmeAnalysis* package can complete tracks which includes gaps in them (Aguet et al., 2013). This is critical to determine accurate lifetimes when weak signals can fluctuate close to the limit of detection (Jaqaman et al., 2008). For example, at the early stages of CME, only a small numbers of proteins are present before they polymerize and produce a brighter stable signal. Our observations indicate that the spots detected in our experiments can be tracked over the length of the movie (Figure 3B). Once the tracking is complete, the fluorescence intensity and lifetime of every particle are examined (Figure 3C). To do this, we extracted the raw tracking output of the *cmeAnalysis* program and used custom made Matlab scripts to screen the trajectories. Tracks that started too close to the start, or to the end, of the movie were excluded to ensure complete recording. Furthermore and as previously described, tracks less than 5 s were excluded to prevent a bias of short tracks caused during the gap linking stage (Aguet et al., 2013). The lifetimes from multiple experiments were combined to produce a robust mean value (Figure 3D). Using the combination of the *cmeAnalysis* algorithm, and our own scripts, for AP2A1-GFP, we calculated a cell surface lifetime of 12.74 s from three different roots and 14,203 individual total tracks. There is very little variation between the different roots imaged (results from experimental replicates were within a range of 1.43 s of each other), therefore demonstrating that our imaging and analysis methods are robust.

To compare our method with a recently published semi-automated analysis method (Higaki, 2015), which is reliant upon ImageJ and human input, we examined a cell expressing AP2A1-GFP using TIRF illumination (Figure 4A) and compared the cell surface lifetime of AP2A1, the number of tracks analyzed, and the time taken to generate results. For the ImageJ analysis, a linear region of interest (ROI) is drawn on the stack image (Figure 4B). This ROI is then resliced to produce a kymograph,

and a Gaussian blur filter applied (Figure 4C). The kymograph is then segmented and the tracks of the particles measured for their length using ImageJ (Figure 4D), as described by Higaki (2015). The results are then copied in to Excel spreadsheet for further processing. This process was repeated six times for the single cell (Figure 4E). Our analysis method successfully automatically detected almost all the particles present in the image and was able to track them over their appearance and disappearance within the movie (Figures 4F,G), requiring human input only for information about the specific imaging setup used. Overall, the cell surface lifetime results were within 1.44 s of each other between the two methods (11.10 and 12.54 s for the ImageJ-based and our own method, respectively) (Figure 4H). There were however striking differences in the number of tracks measured (Figure 4H). Finally, the ImageJ-based method involving a lot more human interaction with the analysis took significantly longer than our method to detect only a limited number of events.

To further validate our method, we examined the cell surface lifetime of DRP1c-GFP, a potential EAP which has been previously reported to have a cell surface lifetime of 17.7 s in developing root tip cells (Konopka et al., 2008). DRP1c-GFP

TABLE 1 | The cell surface lifetime data of DRP1c-GFP was filtered as described by Konopka et al. (2008).

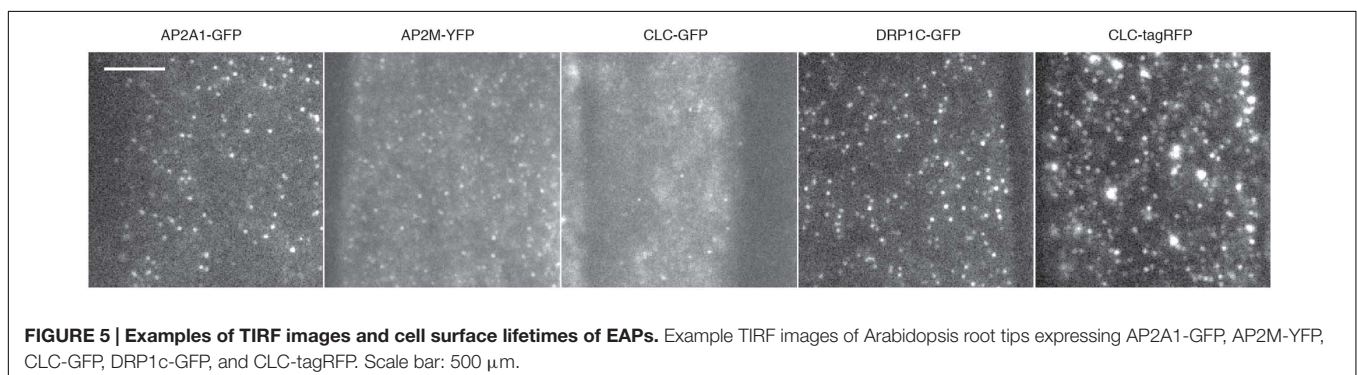
Protein	Tag	Lifetime (s)	$\pm SE$	#Events	#Independent roots
DRP1C	GFP	16.0281	0.1007	53,574	6

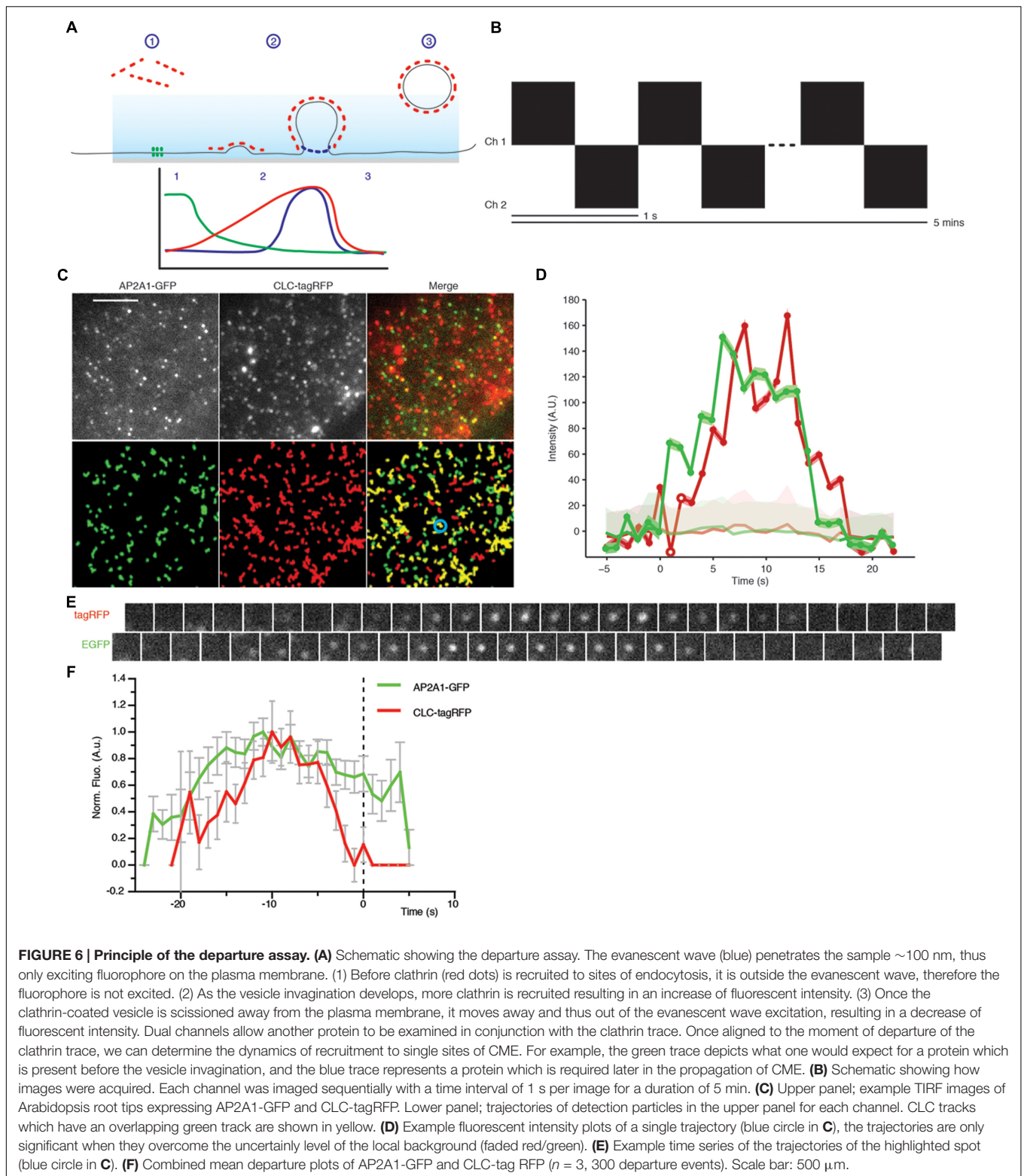
Lifetimes are presented in seconds, and SE represents the standard error to the mean.

TABLE 2 | The cell surface lifetime values of studied EAPs.

Protein	Tag	Lifetime (s)	$\pm SE$	#Events	#Independent roots
AP2A1	GFP	12.553	0.084946	14,203	3
AP2M	YFP	15.87	0.04928	96,228	5
CLC	GFP	10.439	0.067309	16,824	4
DRP1C	GFP	20.305	0.11702	31,420	6
CLC	Tag-RFP	11.671	0.092766	12,449	4

Lifetimes are presented in seconds, and SE represents the standard error to the mean.





formed discrete foci on the cell surface under TIRF illumination (Figure 5), agreeing with previous attempts to image it on the cell surface (Konopka et al., 2008). After detection and tracking, we decided to use the same filtering criteria of the lifetime values

as previously used (Konopka et al., 2008), and found a lifetime of 16.03 s from 53,574 tracks analyzed (Table 1). Further to this, we also examined the lifetimes of clathrin light chain (CLC) tagged with GFP or tagRFP. Both GFP and tagRFP tagged CLC

formed discrete foci on the cell surface (Figure 5), and showed no significant difference in their lifetimes ($p = 0.113$, unpaired t -test; four independent experiments with 16,824 CLC-GFP events and 12,449 CLC-tagRFP events) (Table 2). Therefore, the choice of fluorophore or promoter does not appear to bias cell surface lifetimes in our specific case.

Altogether, this indicated that we successfully established a robust and powerful pipeline to allow TIRF, automated detection, tracking and rapid lifetime calculation of cell surface proteins in root epidermal cells.

Development of a Dual Channel Clathrin Departure Assay in Plants

The physiological significance of single channel cell surface lifetimes is hard to interpret, as it lacks a meaningful physiological context. Without a reference in the experiment to compare the cell surface lifetime to, it is impossible to determine the role of the protein at the cell surface. We therefore developed a dual channel TIRF imaging system using CLC as a reference for CME, where scission of the clathrin-coated vesicle from the membrane is visualized by the sharp decrease of CLC fluorescence (Figure 6A) (Merrifield et al., 2002; Mattheyses et al., 2011). Tracks from the EAP and CLC can be combined from multiple single events of CME and aligned to the moment the CME vesicle departs from the membrane, thus allowing one to define with great precision when EAPs are recruited to single events of CME (Figure 6A).

As a test case for dual TIRF imaging-based departure assay, we monitored the recruitment of AP-2 compared to CLC. Plants expressing AP2A1-GFP were crossed with CLC-tagRFP-expressing plants and the F1 progeny was subjected to this departure assay. Time series movies were captured in both the red and green channels sequentially, with a frequency of 1 s between frames (Figure 6B). Both AP2A1 and CLC formed discrete foci on the cell surface, as expected (Figure 6C). Many more CLC spots were observed at the cell surface compared to AP2A1, consistent with the existence of another adaptor complex in plant that may serve different pools of CME (Gadeyne et al., 2014). Particles in both channels were detected and tracked (Figure 6C), as described above. The raw tracking data was extracted from the *cmeAnalysis* package, and we used homemade Matlab scripts to examine the overlap between CLC and AP2A1 trajectories. Trajectories with an overlap in space and time of 1 frame were paired. From this population of paired trajectories, we then selected trajectories where the CLC lifetime was equal to the mean (± 1 s) of all the CLC trajectories. Paired trajectories where the green track started, or ended more than five frames before or after the red track were discarded, to ensure that only overlapping of trajectories corresponding to a given CME event were analyzed and avoid coincidental overlapping tracks, as previously described (Aguet et al., 2013). The GFP overlapping 'partner' track was then aligned to the moment of the CLC departure (Figures 6D,E). Every departure traces from multiple experiments were normalized and combined to generate a recruitment profile of AP2A1 to sites of CME marked by CLC departure (Figure 6F). The CLC-tagRFP fluorescence trace

is in accordance with the classical model of CME with CLC-tagRFP gradually polymerizing at the cell surface while the vesicle invaginates (indicated by the increase of fluorescence), and then rapidly decreasing as the vesicle moves away from the cell surface (indicated by the decrease in fluorescence). Consistent with the AP-2 being an adaptor for CME driving the recruitment of clathrin to the cell surface (Shih et al., 1995; McMahon and Boucrot, 2011), it arrived at the sites of CME before CLC (Figure 6F). Further to this, AP2A1 shares a similar departure trace as CLC, thus indicating that the AP2A1 subunit is involved in plant CME.

Differential Recruitment of AP-2 Subunits to Sites of CME

AP-2 is the canonical adaptor protein for CME in mammalian systems (McMahon and Boucrot, 2011). AP-2 is a complex made of different subunits, and each subunit appears to play a key role in the propagation of CME. For example, the alpha subunit has cargo recognition sites (i.e., DxF, FxDxF, and WVxF motifs) (Benmerah et al., 1996; Brett et al., 2002; Jha et al., 2004; Walther et al., 2004), and is involved in membrane binding and recruitment of other EAPs (Chen et al., 1998). The beta subunit binds clathrin (Shih et al., 1995), and cargo via the dileucine motif (Hofmann et al., 1999). The mu subunit binds cargo which contain the Yxx Φ (Φ being a bulky hydrophobic residue) motif (Ohno et al., 1995). Many of the subunits are conserved in plants, and overall AP-2 appears to be important for internalization of proteins and development (Chen et al., 2011; Bashline et al., 2013; Di Rubbo et al., 2013; Fan et al., 2013; Kim et al., 2013; Yamaoka et al., 2013). However, AP-2 is not the major adaptor in plants, as deletion still allows production of a viable plant (Bashline et al., 2013; Kim et al., 2013; Yamaoka et al., 2013; Gadeyne et al., 2014). Recent evidence in both plants and *Caenorhabditis elegans* suggests that the AP-2 complex functions as two distinct hemi-complexes

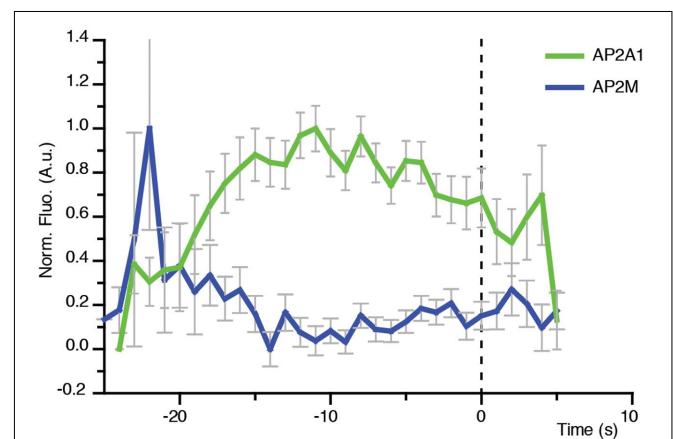


FIGURE 7 | Direct visualization of AP-2 alpha and mu subunits to single sites of CME. Combined mean departure plots of AP2A1-GFP (green) ($n = 3$ cells, 300 departure events) and AP2M-YFP (blue) ($n = 5$ cells, 619 departure events).

composed as alpha/sigma and beta/mu, which have differing partially independent roles (Gu et al., 2013; Wang et al., 2016). Notably, the mu subunit would mediate the recruitment of the alpha subunit to the cell surface (Wang et al., 2016). Consistently, the lifetimes of the alpha and mu subunits at the cell surface were found to be significantly different ($p = 0.0335$, unpaired t -test; AP2A1, $n = 3$ independent experiments with 14,203 events; AP2M, $n = 4$ independent experiments with 96,228 events) (Figure 5).

In contrast to the concomitant recruitment of AP2A1 with CLC (Figure 6F), the recruitment profile of the AP-2 mu subunit at the cell surface only showed a spike prior to the arrival of CLC (Figure 7). This suggests that the AP-2 mu subunit is not required for the propagation of the CME event *per se*, but might in fact be required during the early stages of CME. This agrees with pharmacological and genetic manipulations which showed that loss of the AP-2 mu subunit adversely affected the recruitment of the other AP-2 subunits to the cell surface (Wang et al., 2016).

CONCLUSION

In contrast to routine analysis of cell surface internalization processes performed by traditional confocal and spinning disk microscopy, the utilization of TIRF allows the live and direct examination of the cell surface free from noise, the precise lifetime and departure profile calculation. While TIRF is the imaging approach of choice when examining cell surface processes, there are some limitations. For example, as TIRF is reliant upon the evanescent wave, which typically can only penetrate samples up to 100 nm, the cell of interest must lie flat and in direct contact with the coverslip in order to be illuminated. This restricts the imaging volume of TIRF in intact organisms to only the outside cell layer. Therefore, TIRF is only applicable in plants to certain cell types such as epidermal cells or pollen. It also relies on genetic manipulation of the sample to label the protein of interest with a fluorophore. This could alter the structural properties of how proteins would assemble and interact, further strengthening the necessity to validate the functionality of the fusion protein. While the tagging of clathrin and AP-2 has routinely been done in many systems and shown not to interfere

with their function (Rappoport and Simon, 2008), this has to be established for any new protein imaged. The fluorophore used or the expression level of the tagged proteins imaged however do not seem to influence the cell surface lifetime, at least for clathrin.

Overall, the ability to make precise temporal studies of EAPs is instrumental to reconstitute the sequential events of EAP recruitment and to better characterize endocytosis in plants. With a large body of plant research currently focusing on the dynamics and endocytosis of cell surface receptors and transporters (Luu and Maurel, 2013; Luschnig and Vert, 2014; Zelazny and Vert, 2014; Ben Khaled et al., 2015), TIRF and semi-automated image analysis provide suitable solutions to unravel the molecular mechanisms driving CME, and one's favorite cargo.

AUTHOR CONTRIBUTIONS

AJ and GV: designed the experimental strategy and analyzed data; wrote the manuscript.

FUNDING

This work benefited from the microscopes and expertise of the Imagerie-Gif Cell Biology facility, which is supported by the 'Infrastructures en Biologie Santé et Agronomie' (IBISA), the French National Research Agency under Investments for the Future programmes 'France-BioImaging infrastructure' (ANR-10-INSB-04-01), Saclay Plant Sciences initiative (ANR-10-LABX-0040-SPS) and the 'Conseil Général de l'Essonne'. This work was supported by grants from ATIP program from CNRS, Marie Curie Action (PCIG-GA-2012-334021, to GV) and Agence Nationale de la Recherche (ANR-13-JSV2-0004-01, to GV).

ACKNOWLEDGMENTS

We would like to thank E. Russinova, S. Bednareck, Y. Gu, J. Lin, and D. Van Damme for sharing seeds, and members of the Jaillais lab for critical reading of the manuscript.

REFERENCES

- Aguet, F., Antonescu, C. N., Mettlen, M., Schmid, S. L., and Danuser, G. (2013). Advances in analysis of low signal-to-noise images link dynamin and AP2 to the functions of an endocytic checkpoint. *Dev. Cell* 26, 279–291. doi: 10.1016/j.devcel.2013.06.019
- Axelrod, D. (2001). Total internal reflection fluorescence microscopy in cell biology. *Traffic* 2, 764–774. doi: 10.1034/j.1600-0854.2001.21104.x
- Baisa, G. A., Mayers, J. R., and Bednarek, S. Y. (2013). Budding and braking news about clathrin-mediated endocytosis. *Curr. Opin. Plant Biol.* 16, 718–725. doi: 10.1016/j.pbi.2013.09.005
- Barberon, M., Dubeaux, G., Kolb, C., Isono, E., Zelazny, E., and Vert, G. (2014). Polarization of IRON-REGULATED TRANSPORTER 1 (IRT1) to the plant-soil interface plays crucial role in metal homeostasis. *Proc. Natl. Acad. Sci. U.S.A.* 111, 8293–8298. doi: 10.1073/pnas.1402262111
- Bashline, L., Li, S., Anderson, C. T., Lei, L., and Gu, Y. (2013). The endocytosis of cellulose synthase in arabidopsis is dependent on μ 2, a clathrin-mediated endocytosis adaptin. *Plant Physiol.* 163, 150–160. doi: 10.1104/pp.113.221234
- Ben Khaled, S., Postma, J., and Robatzek, S. (2015). A moving view: subcellular trafficking processes in pattern recognition receptor-triggered plant immunity. *Annu. Rev. Phytopathol.* 53, 379–402. doi: 10.1146/annurev-phyto-080614-120347
- Benmerah, A., Begue, B., Dautry-Varsat, A., and Cerf-Bensussan, N. (1996). The ear of alpha-adaptin interacts with the COOH-terminal domain of the Eps 15 protein. *J. Biol. Chem.* 271, 12111–12116. doi: 10.1074/jbc.271.20.12111
- Brett, T. J., Traub, L. M., and Fremont, D. H. (2002). Accessory protein recruitment motifs in clathrin-mediated endocytosis. *Structure* 10, 797–809. doi: 10.1016/S0969-2126(02)00784-0

- Chen, H., Fre, S., Slepnev, V. I., Capua, M. R., Takei, K., Butler, M. H., et al. (1998). Epsin is an EH-domain-binding protein implicated in clathrin-mediated endocytosis. *Nature* 394, 793–797. doi: 10.1038/28660
- Chen, X., Irani, N. G., and Friml, J. (2011). Clathrin-mediated endocytosis: the gateway into plant cells. *Curr. Opin. Plant Biol* 14, 674–682. doi: 10.1016/j.pbi.2011.08.006
- Dhonukshe, P., Aniento, F., Hwang, I., Robinson, D. G., Mravec, J., Stierhof, Y. D., et al. (2007). Clathrin-mediated constitutive endocytosis of PIN auxin efflux carriers in *Arabidopsis*. *Curr. Biol.* 17, 520–527. doi: 10.1016/j.cub.2007.01.052
- Di Rubbo, S., Irani, N. G., Kim, S. Y., Xu, Z. Y., Gadeyne, A., Dejonghe, W., et al. (2013). The clathrin adaptor complex AP-2 mediates endocytosis of brassinosteroid insensitive1 in *Arabidopsis*. *Plant Cell* 25, 2986–2997. doi: 10.1105/tpc.113.114058
- Fan, L., Hao, H., Xue, Y., Zhang, L., Song, K., Ding, Z., et al. (2013). Dynamic analysis of *Arabidopsis* AP2 sigma subunit reveals a key role in clathrin-mediated endocytosis and plant development. *Development* 140, 3826–3837. doi: 10.1242/dev.095711
- Gadeyne, A., Sanchez-Rodriguez, C., Vanneste, S., Di Rubbo, S., Zauber, H., Vanneste, K., et al. (2014). The TPLATE adaptor complex drives clathrin-mediated endocytosis in plants. *Cell* 156, 691–704. doi: 10.1016/j.cell.2014.01.039
- Gu, M., Liu, Q., Watanabe, S., Sun, L., Holloper, G., Grant, B. D., et al. (2013). AP2 hemicomplexes contribute independently to synaptic vesicle endocytosis. *Elife* 2:e00190. doi: 10.7554/eLife.00190
- Happel, N., Honing, S., Neuhaus, J. M., Paris, N., Robinson, D. G., and Holstein, S. E. (2004). *Arabidopsis* mu A-adaptin interacts with the tyrosine motif of the vacuolar sorting receptor VSR-PS1. *Plant J.* 37, 678–693. doi: 10.1111/j.1365-313X.2003.01995.x
- Higaki, T. (2015). Real-time imaging of plant cell surface dynamics with variable-angle epifluorescence microscopy. *J. Vis. Exp.* 106:e53437. doi: 10.3791/53437
- Hofmann, M. W., Honing, S., Rodionov, D., Dobberstein, B., Von Figura, K., and Bakke, O. (1999). The leucine-based sorting motifs in the cytoplasmic domain of the invariant chain are recognized by the clathrin adaptors AP1 and AP2 and their medium chains. *J. Biol. Chem.* 274, 36153–36158. doi: 10.1074/jbc.274.51.36153
- Jaqaman, K., Loerke, D., Mettlen, M., Kuwata, H., Grinstead, S., Schmid, S. L., et al. (2008). Robust single-particle tracking in live-cell time-lapse sequences. *Nat. Methods* 5, 695–702. doi: 10.1038/nmeth.1237
- Jha, A., Agostinelli, N. R., Mishra, S. K., Keyel, P. A., Hawryluk, M. J., and Traub, L. M. (2004). A novel AP-2 adaptor interaction motif initially identified in the long-splice isoform of synaptotagmin 1. *SJ170. J. Biol. Chem.* 279, 2281–2290. doi: 10.1074/jbc.M305644200
- Kim, S. Y., Xu, Z.-Y., Song, K., Kim, D. H., Kang, H., Reichardt, I., et al. (2013). Adaptor protein complex 2-mediated endocytosis is crucial for male reproductive organ development in *Arabidopsis*. *Plant Cell* 25, 2970–2985. doi: 10.1105/tpc.113.114264
- Kitakura, S., Vanneste, S., Robert, S., Lofke, C., Teichmann, T., Tanaka, H., et al. (2011). Clathrin mediates endocytosis and polar distribution of PIN auxin transporters in *Arabidopsis*. *Plant Cell* 23, 1920–1931. doi: 10.1105/tpc.111.083030
- Konopka, C. A., Backues, S. K., and Bednarek, S. Y. (2008). Dynamics of *Arabidopsis* dynamin-related protein 1C and a clathrin light chain at the plasma membrane. *Plant Cell* 20, 1363–1380. doi: 10.1105/tpc.108.059428
- Langhans, M., and Meckel, T. (2014). Single-molecule detection and tracking in plants. *Protoplasma* 251, 277–291. doi: 10.1007/s00709-013-0601-0
- Loerke, D., Mettlen, M., Yarar, D., Jaqaman, K., Jaqaman, H., Danuser, G., et al. (2009). Cargo and dynamin regulate clathrin-coated pit maturation. *PLoS Biol.* 7:e57. doi: 10.1371/journal.pbio.1000057
- Lu, R., Drubin, D. G., and Sun, Y. (2016). Clathrin-mediated endocytosis in budding yeast at a glance. *J. Cell Sci.* 129, 1531–1536. doi: 10.1242/jcs.182303
- Luschnig, C., and Vert, G. (2014). The dynamics of plant plasma membrane proteins: PINs and beyond. *Development* 141, 2924–2938. doi: 10.1242/dev.103424
- Luu, D.-T., and Maurel, C. (2013). Aquaporin trafficking in plant cells: an emerging membrane-protein model. *Traffic* 14, 629–635. doi: 10.1111/tra.12062
- Martins, S., Dohmann, E. M., Cayrel, A., Johnson, A., Fischer, W., Pojer, F., et al. (2015). Internalization and vacuolar targeting of the brassinosteroid hormone receptor BRI1 are regulated by ubiquitination. *Nat. Commun.* 6:6151. doi: 10.1038/ncomms7151
- Mattheyses, A. L., Atkinson, C. E., and Simon, S. M. (2011). Imaging single endocytic events reveals diversity in clathrin, dynamin and vesicle dynamics. *Traffic* 12, 1394–1406. doi: 10.1111/j.1600-0854.2011.01235.x
- McMahon, H. T., and Boucrot, E. (2011). Molecular mechanism and physiological functions of clathrin-mediated endocytosis. *Nat. Rev. Mol. Cell Biol.* 12, 517–533. doi: 10.1038/nrm3151
- Merrifield, C. J., Feldman, M. E., Wan, L., and Almers, W. (2002). Imaging actin and dynamin recruitment during invagination of single clathrin-coated pits. *Nat. Cell Biol.* 4, 691–698. doi: 10.1038/ncb837
- Merrifield, C. J., and Kaksonen, M. (2014). Endocytic accessory factors and regulation of clathrin-mediated endocytosis. *Cold Spring Harb. Perspect. Biol.* 6:a016733. doi: 10.1101/cshperspect.a016733
- Mettlen, M., and Danuser, G. (2014). Imaging and modeling the dynamics of clathrin-mediated endocytosis. *Cold Spring Harb. Perspect. Biol.* 6:a017038. doi: 10.1101/cshperspect.a017038
- Ohno, H., Stewart, J., Fournier, M. C., Bosshart, H., Rhee, I., Miyatake, S., et al. (1995). Interaction of tyrosine-based sorting signals with clathrin-associated proteins. *Science* 269, 1872–1875. doi: 10.1126/science.7569928
- Rappoport, J. Z. (2008). Focusing on clathrin-mediated endocytosis. *Biochem. J.* 412, 415–423. doi: 10.1042/BJ20080474
- Rappoport, J. Z., and Simon, S. M. (2008). A functional GFP fusion for imaging clathrin-mediated endocytosis. *Traffic* 9, 1250–1255. doi: 10.1111/j.1600-0854.2008.00770.x
- Shih, W., Gallusser, A., and Kirchhausen, T. (1995). A clathrin-binding site in the hinge of the beta 2 chain of mammalian AP-2 complexes. *J. Biol. Chem.* 270, 31083–31090. doi: 10.1074/jbc.270.52.31083
- Viczay-Barrena, G., Webb, S. E. D., Martin-Fernandez, M. L., and Wilson, Z. A. (2011). Subcellular and single-molecule imaging of plant fluorescent proteins using total internal reflection fluorescence microscopy (TIRFM). *J. Exp. Bot.* 62, 5419–5428. doi: 10.1093/jxb/err212
- Walther, K., Diril, M. K., Jung, N., and Haucke, V. (2004). Functional dissection of the interactions of stonin 2 with the adaptor complex AP-2 and synaptotagmin. *Proc. Natl. Acad. Sci. U.S.A.* 101, 964–969. doi: 10.1073/pnas.0307862100
- Wan, Y., Ash, W. M. III, Fan, L., Hao, H., Kim, M. K., and Lin, J. (2011). Variable-angle total internal reflection fluorescence microscopy of intact cells of *Arabidopsis thaliana*. *Plant Methods* 7:27. doi: 10.1186/1746-4811-7-27
- Wang, C., Hu, T., Yan, X., Meng, T., Wang, Y., Wang, Q., et al. (2016). Differential regulation of clathrin and its adaptor proteins during membrane recruitment for endocytosis. *Plant Physiol.* 171, 215–229. doi: 10.1104/pp.15.01716
- Wang, X., Li, X., Deng, X., Luu, D. T., Maurel, C., and Lin, J. (2015). Single-molecule fluorescence imaging to quantify membrane protein dynamics and oligomerization in living plant cells. *Nat. Protoc.* 10, 2054–2063. doi: 10.1038/nprot.2015.132
- Yamaoka, S., Shimono, Y., Shirakawa, M., Fukao, Y., Kawase, T., Hatsugai, N., et al. (2013). Identification and dynamics of *Arabidopsis* adaptor protein-2 complex and its involvement in floral organ development. *Plant Cell* 25, 2958–2969. doi: 10.1105/tpc.113.114082
- Zelazny, E., and Vert, G. (2014). Plant nutrition: root transporters on the move. *Plant Physiol.* 166, 500–508. doi: 10.1104/pp.114.244475
- Zhang, Y., Persson, S., Hirst, J., Robinson, M. S., Van Damme, D., and Sanchez-Rodriguez, C. (2015). Change your TPLATE, change your fate: plant CME and beyond. *Trends Plant Sci.* 20, 41–48. doi: 10.1016/j.tplants.2014.09.002

Conflict of Interest Statement: The authors declare that the research was conducted in the absence of any commercial or financial relationships that could be construed as a potential conflict of interest.

Copyright © 2017 Johnson and Vert. This is an open-access article distributed under the terms of the Creative Commons Attribution License (CC BY). The use, distribution or reproduction in other forums is permitted, provided the original author(s) or licensor are credited and that the original publication in this journal is cited, in accordance with accepted academic practice. No use, distribution or reproduction is permitted which does not comply with these terms.